Constraints on Neutrino Oscillations Using 1258 Days of Super-Kamiokande Solar Neutrino Data

S. Fukuda,[1] Y. Fukuda,[1] M. Ishitsuka,[1] Y. Itow,[1] T. Kajita,[1] J. Kameda,[1] K. Kaneyuki,[1] K. Kobayashi,[1] Y. Koshio,[1] M. Miura,[1] S. Moriyama,[1] M. Nakahata,[1] S. Nakayama,[1] A. Okada,[1] N. Sakurai,[1] M. Shiozawa,[1] Y. Suzuki,[1] H. Takeuchi,[1] Y. Takeuchi,[1] T. Toshito,[1] Y. Totsuka,[1] S. Yamada,[1] S. Desai,[2] M. Earl,[2] E. Kearns,[2] M. D. Messier,[2] K. Scholberg,[2,*] J. L. Stone,[2] L. R. Sulak,[2] C. W. Walter,[2] M. Goldhaber,[3] T. Barszczak,[4] D. Casper,[4] W. Gajewski,[4] W. R. Kropp,[4] S. Mine,[4] D. W. Liu,[4] L. R. Price,[4] M. B. Smy,[4] H. W. Sobel,[4] M. R. Vagins,[4] K. S. Ganezer,[5] W. E. Keig,[5] R. W. Ellsworth,[6] S. Tasaka,[7] A. Kibayashi,[8] J. G. Learned,[8] S. Matsuno,[8] D. Takemori,[8] Y. Hayato,[9] T. Ishii,[9] T. Kobayashi,[9] K. Nakamura,[9] Y. Obayashi,[9] Y. Oyama,[9] A. Sakai,[9] M. Sakuda,[9] M. Kohama,[10] A. T. Suzuki,[10] T. Inagaki,[11] T. Nakaya,[11] K. Nishikawa,[11] T. J. Haines,[12,4] E. Blaufuss,[13,14] S. Dazeley,[13] K. B. Lee,[13,†] R. Svoboda,[13] J. A. Goodman,[14] G. Guillian,[14] G. W. Sullivan,[14] D. Turcan,[14] A. Habig,[15] J. Hill,[16] C. K. Jung,[16] K. Martens,[16,‡] M. Malek,[16] C. Mauger,[16] C. McGrew,[16] E. Sharkey,[16] B. Viren,[16] C. Yanagisawa,[16] C. Mitsuda,[17] K. Miyano,[17] C. Saji,[17] T. Shibata,[17] Y. Kajiyama,[18] Y. Nagashima,[18] K. Nitta,[18] M. Takita,[18] M. Yoshida,[18] H. I. Kim,[19] S. B. Kim,[19] J. Yoo,[19] H. Okazawa,[20] T. Ishizuka,[21] M. Etoh,[22] Y. Gando,[22] T. Hasegawa,[22] K. Inoue,[22] K. Ishihara,[22] T. Maruyama,[22] J. Shirai,[22] A. Suzuki,[22] M. Koshiba,[23] Y. Hatakeyama,[24] Y. Ichikawa,[24] M. Koike,[24] K. Nishijima,[24] H. Fujiyasu,[25] H. Ishino,[25] M. Morii,[25] Y. Watanabe,[25] U. Golebiewska,[26] D. Kielczewska,[26,4] S. C. Boyd,[27] A. L. Stachyra,[27] R. J. Wilkes,[27] and K. K. Young[27,§]

(Super-Kamiokande Collaboration)

[1]*Institute for Cosmic Ray Research, University of Tokyo, Kashiwa, Chiba 277-8582, Japan*
[2]*Department of Physics, Boston University, Boston, Massachusetts 02215*
[3]*Physics Department, Brookhaven National Laboratory, Upton, New York 11973*
[4]*Department of Physics and Astronomy, University of California, Irvine, Irvine, California 92697-4575*
[5]*Department of Physics, California State University, Dominguez Hills, Carson, California 90747*
[6]*Department of Physics, George Mason University, Fairfax, Virginia 22030*
[7]*Department of Physics, Gifu University, Gifu, Gifu 501-1193, Japan*
[8]*Department of Physics and Astronomy, University of Hawaii, Honolulu, Hawaii 96822*
[9]*Institute of Particle and Nuclear Studies, High Energy Accelerator Research Organization (KEK), Tsukuba, Ibaraki 305-0801, Japan*
[10]*Department of Physics, Kobe University, Kobe, Hyogo 657-8501, Japan*
[11]*Department of Physics, Kyoto University, Kyoto 606-8502, Japan*
[12]*Physics Division, P-23, Los Alamos National Laboratory, Los Alamos, New Mexico 87544*
[13]*Department of Physics and Astronomy, Louisiana State University, Baton Rouge, Louisiana 70803*
[14]*Department of Physics, University of Maryland, College Park, Maryland 20742*
[15]*Department of Physics, University of Minnesota, Duluth, Minnesota 55812-2496*
[16]*Department of Physics and Astronomy, State University of New York, Stony Brook, New York 11794-3800*
[17]*Department of Physics, Niigata University, Niigata, Niigata 950-2181, Japan*
[18]*Department of Physics, Osaka University, Toyonaka, Osaka 560-0043, Japan*
[19]*Department of Physics, Seoul National University, Seoul 151-742, Korea*
[20]*International and Cultural Studies, Shizuoka Seika College, Yaizu, Shizuoka 425-8611, Japan*
[21]*Department of Systems Engineering, Shizuoka University, Hamamatsu, Shizuoka 432-8561, Japan*
[22]*Research Center for Neutrino Science, Tohoku University, Sendai, Miyagi 980-8578, Japan*
[23]*The University of Tokyo, Tokyo 113-0033, Japan*
[24]*Department of Physics, Tokai University, Hiratsuka, Kanagawa 259-1292, Japan*
[25]*Department of Physics, Tokyo Institute for Technology, Meguro, Tokyo 152-8551, Japan*
[26]*Institute of Experimental Physics, Warsaw University, 00-681 Warsaw, Poland*
[27]*Department of Physics, University of Washington, Seattle, Washington 98195-1560*

We report the result of a search for neutrino oscillations using precise measurements of the recoil electron energy spectrum and zenith angle variations of the solar neutrino flux from 1258 days of neutrino-electron scattering data in Super-Kamiokande. The absence of significant zenith angle variation and spectrum distortion places strong constraints on neutrino mixing and mass difference in a flux-independent way. Using the Super-Kamiokande flux measurement in addition, two allowed regions at large mixing are found.

For over 30 years, measurements of the solar neutrino flux [1–5] have been significantly below the prediction of the standard solar models (SSMs) [6,7]. Neutrino flavor oscillations, similar to those seen in atmospheric neutrinos [8], are a natural explanation for this discrepancy. This type of flavor conversion is inherently energy dependent. Since Super-Kamiokande (SK) measures the energy of the recoil electron from elastic electron-neutrino scattering, it is sensitive to this energy dependence. In addition to a conversion in vacuum, a matter-induced resonance in the sun [9] may sufficiently enhance the disappearance probability of solar neutrinos even for small neutrino mixing. For some oscillation parameters, matter-enhanced oscillations within the Earth can lead to a different flux during daytime than during the night. Therefore, either a distorted energy dependence or a zenith angle variation of the solar neutrino flux would be considered evidence for oscillation. In addition, the shape of the distortion and zenith angle variation would determine the oscillation parameters independently from uncertainties in the SSM's flux prediction. As a real-time solar neutrino experiment, SK can study the solar zenith angle flux variation.

Super-Kamiokande started taking data in April 1996. It has since confirmed the deficit of solar neutrinos [5], measured the recoil energy spectrum [10], and carried out an initial search for zenith angle variation [11]. In this report, we analyze the first 1258 days of data (31 May 1996 through 6 October 2000) using both spectral distortion and zenith angle variation. The total number of solar neutrino events above a threshold of 5 MeV of recoil electron energy is $18\,464^{+677}_{-590}$. The resulting flux of ^{8}B solar neutrinos, $(2.32^{+0.09}_{-0.08}) \times 10^6$ cm^{-2} s^{-1} [5], is $0.451^{+0.017}_{-0.015}$ of the flux predicted by the reference SSM(BP2000) [6].

The sample is divided into seven zenith angle bins (one day bin and six bins in $\cos\theta_z$ for the night); within each zenith angle bin, the data are divided into eight recoil electron energy bins. We will refer to this way to bin data as the "zenith angle spectrum." We define the zenith angle θ_z of an event as the angle between the vertical direction and the solar direction at the time of the event. Day events have $\cos\theta_z \leq 0$ and night events $\cos\theta_z > 0$. The size of the sample (already divided into seven zenith angles) does not allow a subdivision into 19 energy bins shown in [5]. Because of this statistical limitation the lowest (5.0–5.5 MeV) and the highest (16.0–20.0 MeV) energy bin combine the flux of all zenith angles. Table I shows the flux, statistical, and systematic uncertainty for all zenith angle and energy bins. The expected SSM flux of a particular energy bin is calculated from the total ^{8}B and ^{3}He-proton (hep) flux of BP2000 [6] and the neutrino spectrum from Ortiz et al. [12]. This neutrino spectrum is based on an improved measurement of the β-delayed α spectrum of the ^{8}B decay with a small and well-controlled systematic uncertainty. Earlier reports [10] used the neutrino spectrum by Bahcall et al. [13].

This zenith angle spectrum is analyzed in a two-neutrino oscillation scenario, which can be described with a mixing angle θ and a mass difference Δm^2. We consider two cases: (i) $\nu_e \leftrightarrow \nu_{\mu,\tau}$ and (ii) $\nu_e \leftrightarrow \nu_{\text{sterile}}$. For each set of neutrino oscillation parameters ($\sin^2 2\theta$ and Δm^2) the expected number of solar neutrinos and its zenith angle spectrum are calculated. First, the probability P_1 (P_2) of a solar neutrino to be in the mass eigenstate ν_1 (ν_2) on the surface of the sun is obtained from a numerical calculation which propagates a neutrino wave function from the production point in the core to the surface. This calculation uses models for the distribution of the neutrino production point in the sun [6], the electron density in the sun [6], and the neutrino spectrum [12]. Above $\Delta m^2 = 1.8 \times 10^{-9}$ eV^2 the propagation of the two mass eigenstates from the sun to the Earth and inside the Earth can be assumed to be incoherent. The survival probability at the detector is given by

$$P(\nu_e \rightarrow \nu_e)_{\text{SK}} = P_1 P_{1e} + P_2 P_{2e}, \qquad (1)$$

where P_{1e} (P_{2e}) is the probability to be ν_e at the detector if the neutrino arrives at the Earth as ν_1 (ν_2) taking into account matter effects inside the Earth [9]. The electron density model for the Earth (PREM [14]) assumes a charge-to-mass ratio (Z/A) of 0.468 for the core and 0.497 for the mantle [15]. Below $\Delta m^2 = 1.8 \times 10^{-9}$ eV^2 matter effects inside the Earth are unimportant and the propagation from the sun to the Earth is assumed to be coherent. The survival probability is then

$$P(\nu_e \rightarrow \nu_e)_{\text{SK}} = P_1 \cos^2\theta + P_2 \sin^2\theta$$
$$+ 2 \times \sqrt{P_1 P_2} \cos\theta \sin\theta \cos\left(\frac{\Delta m^2 L}{2E_{\nu_e}}\right),$$
$$(2)$$

where L is the distance from the sun to the Earth ranging from perihelion (winter) to aphelion (summer) [16].

Four experiments have published measurements of the solar neutrino flux: Homestake [1] ($2.56 \pm 0.16 \pm 0.16$ SNU), SAGE [3] ($75.4^{+7.8}_{-7.4}$ SNU), GALLEX/GNO [4] ($74.1^{+6.7}_{-6.8}$ SNU), and SK [5]. Taking an average of SAGE and GALLEX, a combined analysis results in several allowed regions. The combined analysis is performed by the method given in [17] considering updated theoretical correlated and uncorrelated uncertainties (^{37}Cl cross section [13], ^{71}Ga cross section [18], neutrino-electron scattering cross section [19], and diffusion [20]). The crosshatched areas of Fig. 1 show the allowed regions at 95% C.L. ($\chi^2 < \chi^2_{\text{min}} + 5.99$) assuming $\nu_e \rightarrow \nu_{\mu,\tau}$ oscillation. There are four allowed regions called "small mixing angle solution" (SMA, $\Delta m^2 \approx 10^{-5}$ eV^2, $\sin^2 2\theta \approx 10^{-2}$–$10^{-3}$), "large mixing angle solution" (LMA, $\Delta m^2 \approx 10^{-4}$–$10^{-5}$ eV^2, $\sin^2 2\theta > 0.5$), "low solution" (LOW, $\Delta m^2 \approx 10^{-7}$ eV^2, $\sin^2 2\theta \approx 0.9$) [21], and "just-so solution" ($\Delta m^2 < 10^{-9}$ eV^2). The SMA and just-so solutions predict spectral distortion, while the LMA and LOW solutions predict a zenith angle variation and can therefore be constrained by the zenith angle spectrum data of SK. The crosshatched areas of Fig. 2 are the combined analysis allowed regions at 95% C.L. assuming $\nu_e \leftrightarrow \nu_{\text{sterile}}$ oscillation. In this case, LMA and

TABLE I.   Flux, uncertainty, and definition of zenith angle and energy bins. The systematic uncertainty in the last two columns is split into energy-uncorrelated and energy-correlated uncertainty. The systematic uncertainty is assumed to be fully correlated in the zenith angle.

	Flux ± statistical uncertainty in units of SSM							Syst. uncert. in %	
	Day	Mantle 1	Mantle 2	Mantle 3	Mantle 4	Mantle 5	Core	Energy	
$\cos\theta_z$-Range	$-1.00-0.00$	$0.00-0.16$	$0.16-0.33$	$0.33-0.50$	$0.50-0.67$	$0.67-0.84$	$0.84-1.00$	Uncorr.	Correlated
5.0–5.5 MeV				0.436 ± 0.046				$+3.9$ -3.1	$+0.25$ -0.21
5.5–6.5 MeV	0.431 ± 0.022	0.464 ± 0.060	0.410 ± 0.055	0.442 ± 0.048	0.453 ± 0.048	0.495 ± 0.054	0.434 ± 0.058	$+1.5$ -1.4	$+0.30$ -0.26
6.5–8.0 MeV	0.461 ± 0.013	0.524 ± 0.036	0.506 ± 0.033	0.438 ± 0.028	0.466 ± 0.027	0.424 ± 0.030	0.409 ± 0.033	± 1.4	$+0.77$ -0.75
8.0–9.5 MeV	0.437 ± 0.014	0.449 ± 0.038	0.482 ± 0.036	0.460 ± 0.031	0.503 ± 0.031	0.461 ± 0.034	0.439 ± 0.037	± 1.4	± 1.6
9.5–11.5 MeV	0.434 ± 0.015	0.432 ± 0.042	0.493 ± 0.040	0.446 ± 0.034	0.448 ± 0.034	0.435 ± 0.037	0.484 ± 0.044	± 1.4	$+3.1$ -2.9
11.5–13.5 MeV	0.456 ± 0.026	0.496 ± 0.071	0.290 ± 0.055	0.394 ± 0.053	0.477 ± 0.056	0.439 ± 0.061	0.465 ± 0.068	± 1.4	$+5.5$ -5.0
13.5–16.0 MeV	0.482 ± 0.056	0.532 ± 0.155	0.775 ± 0.171	0.685 ± 0.141	0.607 ± 0.130	0.471 ± 0.128	0.539 ± 0.153	± 1.4	$+9.2$ -8.3
16.0–20.0 MeV				0.476 ± 0.149				± 1.4	$+16$ -14

LOW solutions do not occur, since there is not enough neutral current contribution to neutrino-electron scattering to accommodate the difference between the SK and the Homestake flux results.

Using the zenith angle spectrum the probability of two neutrino oscillation scenarios was tested with a χ^2 method. For each energy bin i, we form a zenith angle flux difference vector $\vec{\Delta}_i$. Its seven zenith components $\Delta_{i,z}$ are

$$\Delta_{i,z} = \frac{\phi_{i,z}^{\mathrm{meas}}}{\phi_i^{\mathrm{SSM}}} - \alpha \times f(E_i, \delta_{\mathrm{corr}}) \times \frac{\phi_{i,z}^{\mathrm{osc}}}{\phi_i^{\mathrm{SSM}}},$$

where z is the zenith angle bin, $\phi_{i,z}^{\mathrm{meas}}$ is the observed flux of each energy and zenith angle bin, and ϕ_i^{SSM} and $\phi_{i,z}^{\mathrm{osc}}$ are the expected event rates in that bin without and with neutrino oscillation. The spectral distortion f due to the correlated systematic error (see Table I) of $\phi_{i,z}$ is scaled by the parameter δ_{corr}. The definition of the χ^2 is thus

$$\chi^2 = \sum_{i=1}^{8} \vec{\Delta}_i \cdot V_i^{-1} \cdot \vec{\Delta}_i + \left(\frac{\delta_{\mathrm{corr}}}{\sigma_{\mathrm{corr}}} \right)^2. \qquad (3)$$

Each energy bin i has also a separate 7×7 error matrix V_i describing the energy-uncorrelated uncertainty. V_i is
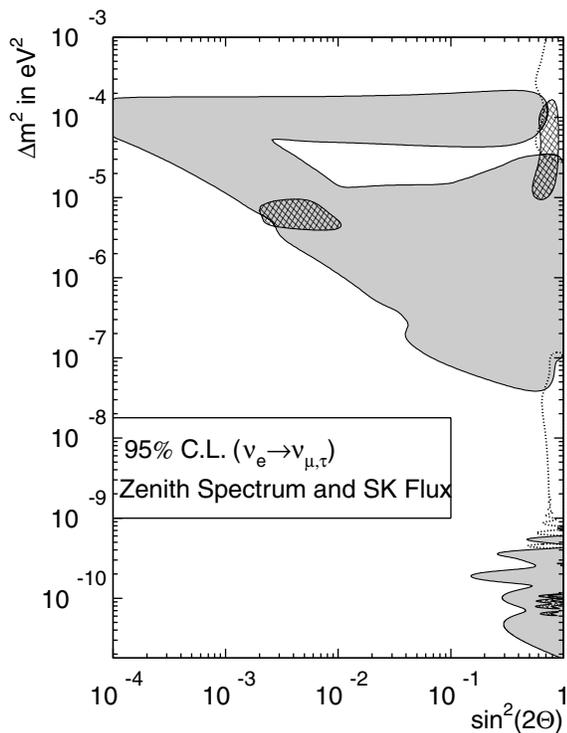
FIG. 1.   Exclusion area for two-flavor oscillation $\nu_e \leftrightarrow \nu_\mu/\nu_\tau$ from (flux-independent) zenith angle spectrum analysis at 95% confidence level (gray areas). Overlaid are the allowed areas (95% C.L.) obtained by the flux-constraint analysis using the zenith angle spectrum and the SSM flux prediction (inside dotted lines). The crosshatched areas are allowed at 95% in a combined fit based only on the absolute fluxes measured at GALLEX [4], SAGE [3], Homestake [1], and Super-Kamiokande [5].
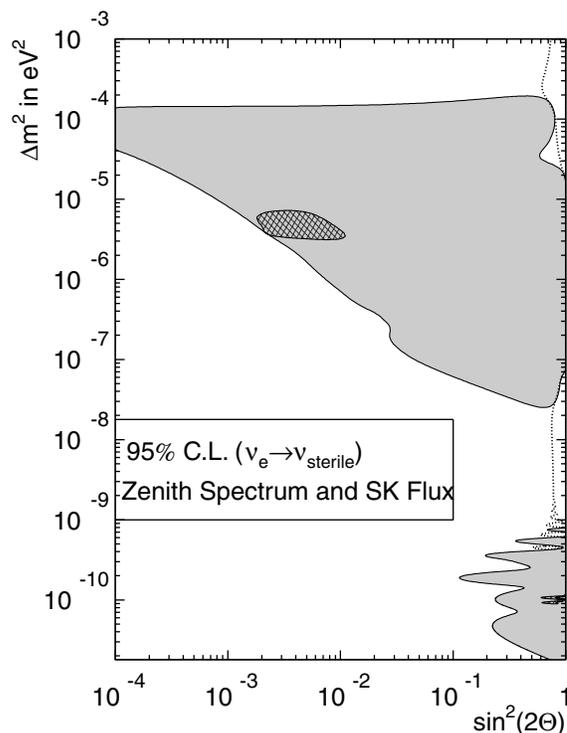
FIG. 2.   Exclusion and allowed areas (defined as in the active case in Fig. 1) for two-flavor oscillation $\nu_e \leftrightarrow \nu_{\mathrm{sterile}}$.

the sum of the statistical error matrix and the energy-uncorrelated systematic error matrix (see Table I), the latter of which is constructed assuming full correlation in zenith angle. The flux normalization factor α is unconstrained to make the χ^2 independent of the total solar neutrino flux. The correlation parameter δ_{corr} is constrained within σ_{corr}. The size and shape of the correlated error are calculated as in [10]. The hep contribution to the neutrino flux is not constrained.

The χ^2 values are calculated in the parameter space $(10^{-4} \leq \sin^2 2\theta \leq 1, \quad 10^{-11} \text{ eV}^2 \leq \Delta m^2 \leq 10^{-3} \text{ eV}^2)$. In the case of active neutrinos, the minimum χ^2 value is 36.1 with 40 degrees of freedom at $(\sin^2 2\theta = 1, \Delta m^2 = 6.53 \times 10^{-10} \text{ eV}^2)$. The best-fit flux normalization is $\alpha = 0.788$, the correlation parameter is $\delta_{corr} = -0.06\sigma_{corr}$, and the hep flux is 0. The shaded areas in Fig. 1 are excluded at 95% C.L. from this flux-independent analysis. Most of the SMA and just-so solutions are disfavored with this C.L. In the case of sterile neutrinos, the minimum χ^2 value is 35.7 at $(\sin^2 2\theta = 1, \Delta m^2 = 6.57 \times 10^{-10} \text{ eV}^2)$. All possible solutions are disfavored at 95% C.L. in this case. The best-fit flux normalization is $\alpha = 0.917$, the correlation parameter is $\delta_{corr} = 0.06\sigma_{corr}$, and the hep flux is 0. The shaded areas in Fig. 2 show the excluded regions (95% C.L.).

Using the theoretical uncertainty of the ^{8}B flux $\sigma_{flux} = {}^{+0.20}_{-0.16}$SSM, an analysis combining flux and zenith angle spectrum has also been performed. In the active neutrino case, the minimum χ^2 value is 37.8 with 41 d.o.f. at the same position as the unconstrained case. The flux normalization changes to $\alpha = 0.789$ and the correlation parameter to $\delta_{corr} = -0.02\sigma_{corr}$. Some LMA χ^2 are similar to the minimum. For example, $\chi^2 = 39.1$ at $(\sin^2 2\theta = 0.87, \Delta m^2 = 7 \times 10^{-5} \text{ eV}^2)$ with a hep flux of $2.9 \times$ BP2000. The dotted lines in Fig. 1 show the contours of the 95% C.L. allowed regions. In the sterile neutrino case, the minimum χ^2 value is 35.9 with 41 d.o.f at the same position as the unconstrained case. Flux normalization, correlation parameter, and hep flux are unchanged. The area inside the dotted lines in Fig. 2 is allowed at 95% C.L. Since the allowed area from the combined flux analysis does not overlap these regions, oscillations into only sterile neutrinos are disfavored at this confidence level.

Figures 1 and 2 are based on the χ^2 analysis of the zenith angle spectrum. We have also performed an oscillation search using the "day/night spectrum," which, in contrast to the zenith angle spectrum, divides the data into two zenith angle bins (day and night bin). Each of these bins is then divided into 19 energy bins [5]. The χ^2 is defined as follows:

$$\chi^2 = \sum_{D,N} \sum_{i=1}^{19} \left(\frac{\Delta_{i,D/N}}{\sigma_i} \right)^2 + \left(\frac{\delta_{corr}}{\sigma_{corr}} \right)^2.$$

The notation is analogous to that used in the χ^2 definition of the zenith angle spectrum analysis. σ_i is the sum of statistical and uncorrelated errors added in quadrature.

The minimum χ^2 value is 28.2 with 34 degrees of freedom at $\sin^2 2\theta = 0.4$ and $\Delta m^2 = 1.38 \times 10^{-10} \text{ eV}^2$. The best-fit flux normalization is $\alpha = 0.488$, the correlation parameter is $\delta_{corr} = -0.2\sigma_{corr}$, and the hep flux is 18 times the SSM flux. Figure 3 shows the 95% excluded regions using the shape of this day/night spectrum. The excluded area is similar to that obtained from the zenith angle spectrum, but more restrictive in the SMA region. The lower left corner of the SMA predicts a slight depression of the core flux resulting in a day flux prediction that is larger than the night flux. SK measures a 1.3σ excess of the night flux over the day flux [5], but the flux in the core bin is below the day flux. This leads to a slightly better fit of these parameters to the zenith angle spectrum than to the day/night spectrum. The lower left corner of the SMA 95% C.L. region is excluded at 93% C.L. by the zenith angle spectrum and at 97% C.L. by the day/night spectrum analysis. The excluded area of the zenith angle spectrum at the LMA and near the LOW solution is larger because of predicted zenith angle variations within the night bin. Other differences are due to the use of different energy bins.

In summary, Super-Kamiokande has precisely measured the energy dependence and zenith angle dependence of the solar ^{8}B neutrino flux. The data do not show a significant distortion of the spectrum or zenith angle variation. This places strong constraints on neutrino oscillation solutions to the solar neutrino problem independently of the flux expectation. If oscillations into active neutrinos are
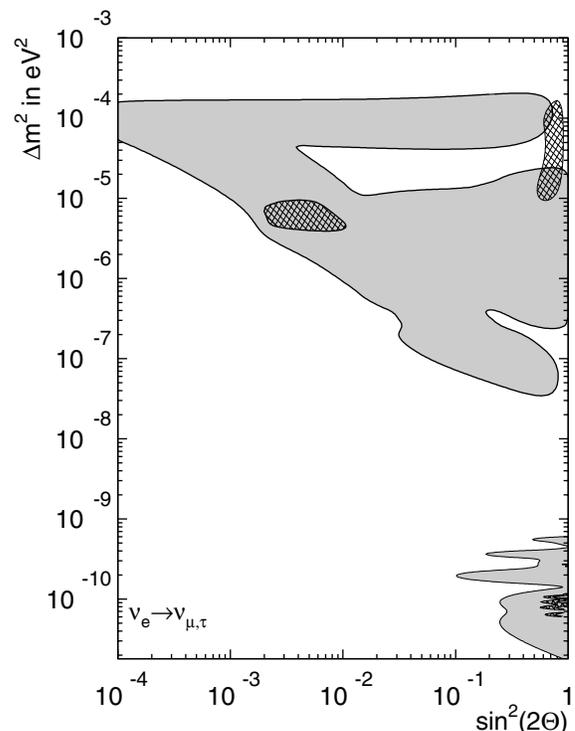
FIG. 3.   Exclusion area for two-flavor oscillation $\nu_e \leftrightarrow \nu_\mu / \nu_\tau$ from a day/night spectrum analysis. As in Fig. 1, the cross-hatched area is allowed at 95% C.L. by the combined flux analysis.

assumed, just-so and the SMA solutions are disfavored at 93% (zenith angle spectrum) to 97% C.L. (day/night spectrum) and the LMA solutions are preferred. All possible oscillation solutions into only sterile neutrinos are disfavored at the 95% confidence level.

In conjunction with the SK ^{8}B flux measurement, two allowed areas at large mixing remain. For the active neutrino case, one of these allowed areas overlaps with the LMA solution, the other one stretches from 10^{-7} to 10^{-10} eV^2. For the sterile neutrino case, there is no overlap with the areas allowed by the rate measurements from the four experiments.

---

*Present address: Department of Physics, Massachusetts Institute of Technology, Cambridge, MA 02139.

†Present address: Korea Research Institute of Standards and Science, Yusong P.O. Box 102, Taejon, 305-600, Korea.

‡Present address: Department of Physics, University of Utah, Salt Lake City, UT 84112.

§Deceased.

[1] B. T. Cleveland et al., Astrophys. J. 496, 505 (1998).

[2] Y. Fukuda et al., Phys. Rev. Lett. 77, 1683 (1996).

[3] V. Gavrin, Nucl. Phys. B (Proc. Suppl.) 91, 36 (2001); J. N. Abdurashitov et al., Phys. Lett. B 328, 234 (1994).

[4] E. Bellotti, Nucl. Phys. B (Proc. Suppl.) 91, 44 (2001); W. Hampel et al., Phys. Lett. B 388, 364 (1996); P. Anselmann et al., Phys. Lett. B 342, 440 (1995).

[5] S. Fukuda et al., preceding Letter, Phys. Rev. Lett. 86, 5651 (2001).

[6] J. N. Bahcall et al., astro-ph/0010346. The ^{8}B flux we have used is 5.15×10^6 cm^{-2} s^{-1}. After this paper was prepared we were informed that the ^{8}B flux has been updated to 5.05×10^6 cm^{-2} s^{-1} in BP2000. This update does not change our conclusions.

[7] S. Turck-Chièze and I. Lopes, Astrophys. J. 408, 347 (1993).

[8] Y. Fukuda et al., Phys. Rev. Lett. 81, 1562 (1998).

[9] S. P. Mikheyev and A. Y. Smirnov, Sov. J. Nucl. Phys. 42, 913 (1985); L. Wolfenstein, Phys. Rev. D 17, 2369 (1978).

[10] Y. Fukuda et al., Phys. Rev. Lett. 82, 2430 (1999).

[11] Y. Fukuda et al., Phys. Rev. Lett. 82, 1810 (1999).

[12] C. E. Ortiz et al., Phys. Rev. Lett. 85, 2909 (2000).

[13] J. N. Bahcall et al., Phys. Rev. C 54, 411 (1996).

[14] A. M. Dziewonski and D. L. Anderson, Phys. Earth Planet. Inter. 25, 297 (1981).

[15] J. N. Bahcall and P. I. Krastev, Phys. Rev. C 56, 2839 (1997).

[16] In the case of vacuum oscillations $P_1 = \cos^2\theta$, $P_2 = \sin^2\theta$, and this reduces to $1 - \sin^2 2\theta \sin^2 \frac{\Delta m^2 L}{4E}$.

[17] G. L. Fogli and E. Lisi, Astropart. Phys. 3, 185 (1995).

[18] J. N. Bahcall, Phys. Rev. C 56, 3391 (1997).

[19] J. N. Bahcall, M. Kamionkowski, and A. Sirlin, Phys. Rev. D 51, 6146 (1995).

[20] J. N. Bahcall and M. Pinsonneault, Rev. Mod. Phys. 67, 781 (1995).

[21] This solution appears only at 99% C.L.; however, it is usually discussed as a possible solution.